

1 **Supplementary Methods**

2 **Chemicals, Peptides, and Recombinant Proteins**

3 Caerulein (Cayman, Cat#24408), Gemcitabine (Teva Parenteral Medicine
4 Inc, Cat#NDC0703-5778-01), Aminooxyacetic acid (AOA; MedChemExpress,
5 Cat#HY-107994), BPTES (Sigma-Aldrich, Cat#SML0601), EGCG (Cayman,
6 Cat#70935), Matrigel Matrix (Corning, Cat#354234), [U-¹³C₅] glutamine
7 (Cambridge Isotope Laboratories, Cat# CLM-1822-H-PK), DAPI (Invitrogen,
8 Cat#P36935), Hematoxylin (Leica, Cat#3801570), Alcoholic Eosin (Leica,
9 Cat#3801615), Turbofect transfection reagent, (Thermo Fisher, Cat#R0532),
10 Dispase II (Sigma-Aldrich, Cat#D4693), TRIzol (Thermo Fisher,
11 Cat#15596026), Pierce IP Lysis Buffer (Thermo Fisher, Cat#87788), Epitope
12 Retrieval Solution (pH 6; Leica, Cat#6064204), PowerUP SYBR Green
13 Mastermix (Applied Biosystems, Cat#A25742), 3-[4,5-dimethylthiazol-2-yl]-2,5-
14 diphenyltetrazolium bromide (MTT; Sigma Aldrich, Cat#M2128), Nonidet P-40
15 (Sigma Aldrich, Cat#74385-1L), Tris-HCl (Sigma Aldrich, Cat#T5941-500G),
16 EDTA (Sigma Aldrich, Cat#E6758-500G), SRT2104 (MedChemExpress,
17 Cat#HY-15262), Honokiol (Sigma-Aldrich, Cat#42612), Skim Milk (BD Difco,
18 Cat#232100), B-27™ Supplement (Thermo Fisher, Cat#17504044), PGE2
19 (Sigma-Aldrich, Cat#A0409-1MG), Nicotinamide (Sigma-Aldrich, Cat#A0636-
20 100G), N-acetylcysteine (Sigma-Aldrich, Cat#A9165-100G), hGastrin I
21 (TOCRIS, Cat#3006), hFGF10 (PeproTech, Cat#100-26), mNoggin
22 (PeproTech, Cat#250-38), hEGF (PeproTech, Cat# AF-100-15), A 83-01
23 (TOCRIS, Cat#2939), DMEM/F12 (Sigma-Aldrich, Cat#DF-041), HEPES
24 (Sigma-Aldrich, Cat#H4034), Matrigel (Corning, Cat#354234), Y-27632 (Hello
25 Bio, Cat#HB2297), Collagenase XI (Sigma-Aldrich, Cat#C7657-25MG), DNase
26 I (Sigma-Aldrich, Cat#11284932001).

27

28 **Commercial Assays**

29 CellTiter-Glo cell Viability Assay Kit (Promega, Cat#G7570), Verso cDNA
30 Synthesis Kit (Thermo Fisher Scientific, Cat#1453A), VetScan Comprehensive
31 Diagnostic Profile (Abaxis, Cat#500-0038-48), Plasmid Maxi kit (Qiagen,
32 Cat#12163), Vectastain ABC Kit (Vector Biolabs, Cat#PK6101), DAB Substrate
33 Kit (Vector Biolabs, Cat#SK-4105), Alcian Blue Stain Kit (IHC World, Cat#IW-
34 3000), GOT Activity Assay Kit (Sigma Aldrich, Cat#MAK055), Glutaminase
35 Activity Assay Kit (Biomedical Research Service, Cat#E-133), GDH Activity
36 Assay Kit (Biomedical Research Service, Cat#E-123), KOD-Plus-Mutagenesis
37 Kit (Toyobo, Cat#SMK101), SIRT1 Activity Assay Kit (Abcam, Cat#ab156065),
38 SIRT3 Activity Assay Kit (Abcam, Cat#ab156067), SIRT5 Activity Assay Kit
39 (Abcam, Cat#ab210074), Mycoplasma PCR Detection Kit (abm, Cat#G238).

40

41 **Organoid Culture and Experiments**

42 The detailed procedure for generating organoids was performed as
43 previously identified ¹. In brief, the tissue from the patient-derived xenografts
44 (PDX) were minced and then incubated in the digestion media (Human
45 Complete Medium containing 10 µg/mL DNase I, 1 mg/mL Collagenase XI,
46 10.5 µM Y-27632) at 37°C with gentle rotation for 1 hour. Cells were collected
47 and then seeded with Matrigel (cat#354234, Corning). The organoids were
48 cultured in Human Complete Feeding Medium (advanced DMEM/F12
49 containing 10 mM HEPES, 1X Glutamax, 500 nM A83-01, 50 ng/mL hEGF, 100
50 ng/mL mNoggin, 100 ng/mL hFGF10, 0.01 µM hGastrin I, 1.25 mM N-
51 acetylcysteine, 10 mM nicotinamide, 1 µM PGE2, 1X B27 supplement, 10% R-
52 spondin1 conditioned media, and 50% Wnt3A-conditioned media). For the
53 indicated experiments, 2×10^3 organoid cells were suspended in 50 µL Matrigel
54 per well and seeded in 24 well plates. Cytation 3 Cell Imaging Multi-Mode
55 Reader was used to capture the size of the organoids. CellTiter-Glo kit
56 (Promega; Madison, WI, USA) was used to measure the cell viability of
57 organoids 72-hours post-treatment.

58

59 ***In Vivo* Mouse Studies**

60 We utilized the following mice strains: Athymic *Foxn1^{nu}/Foxn1^{nu}* (Taconic
61 Biosciences), C57BL/6 (The Jackson Laboratory), NOD scid gamma (NSGTM;
62 The Jackson Laboratory), *Sirt5^{flox/flox}* (Provided by Dr. Johan Auwerx), *LSL-
63 Kras^{G12D/+}* (NCI), *LSL-Trp53^{R172H/+}* (NCI), *Pdx-1-Cre* (NCI). All animal
64 experiments were conducted under the protocols approved by the institutional
65 animal care and use committee (IACUC) at the University of Nebraska Medical
66 Center (UNMC). The animal facility of UNMC bred and housed the athymic
67 nude mice (*Foxn1^{nu}/Foxn1^{nu}*) as well as the NOD *scid* gamma (NSGTM;
68 NOD.Cg-*Prkdc^{scid} Il2rg^{tm1Wjl}/SzJ*) mice used for orthotopic implantations. For
69 the *in vivo* tumor growth experiments, 5×10^5 T3M4-shScramble or T3M4-
70 shSIRT5 cells were injected into the pancreatic tissue of six-week-old female
71 NOD-SCID mice. After 6 days following implantation, tumor diameters were
72 measured by calipers every three days, and tumor volumes were calculated
73 using the following formula: volume = $0.5 \times (\text{longer diameter} \times \text{shorter}$
74 $\text{diameter}^2)$. For the AOA treatment studies, 2×10^6 T3M4-shScramble and
75 T3M4-shSIRT5 were injected into the pancreas of eight-week-old female nude
76 mice. When the tumor size reached approximately 100 mm³, the mice were
77 randomized into the following two groups: vehicle control group (saline) and
78 AOA group, which was treated daily with 10 mg/kg AOA. Body weight and tumor
79 volume were measured twice a week during the treatment. At the end of
80 treatment, mice were euthanized to collect tumor weight and tumor volume.
81 Mice organs and tumor tissues were excised, frozen in liquid nitrogen or fixed
82 with 4% paraformaldehyde, and embedded in paraffin for further analysis.

83

84 **Patient-Derived Xenograft (PDX) Studies**

85 Eight to ten weeks old male NOD *scid* gamma (NSGTM; NOD.Cg-*Prkdc*^{*scid*}
86 *Il2rg*^{*tm1Wjl*}/SzJ) mice were used to implant orthotopic PDX tumors. The PDX
87 (PA137) tumors were cut into 3-5 mm pieces and then orthotopically implanted
88 to the mouse pancreas. When the tumor size reached around 100 mm³, mice
89 were randomized into four groups with similar tumor volumes: control group,
90 gemcitabine (diluted in saline, 25 mg/kg, twice per week), MC3138 [diluted in
91 DMSO: corn oil (1:9) solution, 200 mg/kg, daily] and gemcitabine with MC3138.
92 Gemcitabine and MC3138 were administered by intraperitoneal injections. and
93 gemcitabine with MC3138. Blinding was not possible for the mouse studies.
94 Tumor diameters and body weight were measured every four days. After 20
95 days of treatment, mice were euthanized to collect tumor weight and tumor
96 volume. Mice organs and tumor tissues were excised, frozen in liquid nitrogen
97 or fixed with 4% paraformaldehyde, and embedded in paraffin for further
98 analysis.

99

100 **RNA Extraction and qRT-PCR Analysis**

101 Total RNA from cell lines and tissues were extracted using TRIzol reagent.
102 Reverse transcription analyses used the Verso-cDNA synthesis kit, according
103 to the manufacturer's instructions. QuantStudio 5 Real-Time PCR System
104 (Thermo Fisher Scientific; Waltham, MA, USA) and SYBR Green PCR Master
105 Mix were used to perform the qPCR according to the manufacturer's protocol.
106 Quantification of target genes was normalized by 18S ribosomal RNA using the
107 2- $\Delta\Delta$ Ct method ². The primer sequences used for qPCR analysis are listed in
108 Supplementary Table S4.

109

110 **Antibodies**

111 Rabbit Anti-SIRT5 (HPA022002; RRID: AB_1856913; Sigma-Aldrich),
112 Rabbit Anti-Amylase (A8273; AB_258380; Sigma-Aldrich), Rabbit Anti-
113 cytokeratin19 (TROMA-III; RRID: AB_2133570; DHSB), Rabbit Anti-
114 Glutaminase (ab93434; RRID: AB_10561964; Abcam), Rabbit Anti-Glutamate
115 Dehydrogenase, (12793; RRID: AB_2750880; Cell Signaling Technology),
116 Mouse Anti- β -actin (JLA20; RRID: AB_528068; DHSB), Rabbit Anti-GOT1
117 (HPA072629; RRID: AB_2686540; Sigma-Aldrich), Rabbit Anti-GOT1 (14886-
118 1-AP, RRID:AB_2113630; Thermo Fisher), Rabbit Anti-GOT2 (ab171739;
119 Abcam), Rabbit Anti-Cleaved Caspase3 (9664; RRID: AB_2070042; Cell
120 Signaling Technology), Rabbit Anti-Ki67 (12202; RRID: AB_2620142; Cell
121 Signaling Technology), Rabbit Pan anti-succinyllysine (PTM401; RRID:
122 AB_2687628; PTM Biolabs), Rabbit Pan anti-malonyllysine (PTM901; RRID:
123 AB_2687947; PTM Biolabs), Rabbit Pan anti-glutaryllysine (PTM1151; PTM
124 Biolabs), Rabbit Pan anti-acetylated-lysine (9441; RRID: AB_331805; Cell
125 Signaling Technology), Pierce Anti-HA Magnetic Beads (Cat#88837; Thermo

126 Fisher Scientific), Pierce Protein A/G Magnetic Beads (88803; Thermo Fisher
127 Scientific), Donkey Anti-Rabbit Af594 (711-585-152; RRID: AB_2340621;
128 Jackson Immunoresearch), Donkey Anti-Rat Af488 (712-545-153; RRID:
129 AB_2340684; Jackson Immunoresearch), IgG Fraction, mouse anti-rabbit, light
130 chain specific (211-002-171;RRID: AB_2339146; Jackson Immunoresearch),
131 HA antibody (MMS-101R; RRID: AB_291262; Covance), Peroxidase AffiniPure
132 Goat Anti-Mouse IgG, light chain specific (115-035-174; AB_2338512; Jackson
133 Immunoresearch).

134

135 **Immunoblotting**

136 Cell lysates were extracted from cell culture dishes in RIPA lysis buffer
137 (50mM Tris-HCl pH 8.0 containing 150mM NaCl, 1% Nonidet P-40, 5mM EDTA
138 and 1mM phenylmethylsulphonyl fluoride). Protein samples were separated by
139 sodium dodecyl sulphate-polyacrylamide gel electrophoresis (SDS-PAGE) and
140 transferred to polyvinylidene fluoride (PVDF) membranes. The membranes
141 were blocked with 5% skim milk and then probed overnight at 4°C with indicated
142 primary antibodies. After incubation with horseradish peroxidase (HRP)
143 conjugated secondary antibodies, the specific protein bands were detected
144 using Pierce™ ECL Western Blotting Substrate and ChemiDoc Imaging
145 System (Bio-Rad; Hercules, CA, USA). Immunoblotting assays to detect
146 acetylation levels of purified GOT1 protein used the light-chain specific
147 secondary antibody.

148 **Immunoprecipitation (IP) and Proteomic Analysis**

149 The indicated PDAC cells transfected with HA-GOT1 for 48h were lysed in
150 Pierce™ IP Lysis Buffer (87787, Thermo Fisher). Cell lysates were pre-cleared
151 by Pierce™ Protein A/G Magnetic Beads and then incubated with anti-HA
152 Magnetic Beads overnight at 4°C. After washing with IP Lysis Buffer five times
153 and subsequently boiling with 2X sample buffer for 10 minutes, the GOT1-IP
154 samples were then purified and resolved by SDS-PAGE. Following the
155 Coomassie Brilliant Blue staining and in-gel digestion, the GOT1 peptide
156 mixture was processed for proteomic analysis by LC-MS/MS at the Mass
157 Spectrometry and Proteomics Core at UNMC. For cells expressing wild-type
158 GOT1, K276R, K290R, and K369R mutant GOT1, cells were lysed in IP Lysis
159 Buffer and then pre-cleared by Pierce™ Protein A/G Magnetic Beads. After
160 incubating the pre-cleared lysates with anti-HA Magnetic Beads overnight at
161 4°C, the immune complexes were resolved by SDS-PAGE, followed by
162 immunoblotting analysis. For endogenous IP, control and *SIRT5*-knockdown
163 PDAC cells were lysed in Pierce™ IP Lysis Buffer. The IP-grade GOT1
164 antibody (14886-1-AP, Thermo Fisher) was conjugated to Pierce™ Protein A/G
165 Magnetic Beads at 4°C for four hours before IP experiment. Cell lysates were
166 pre-cleared by Pierce™ Protein A/G Magnetic Beads and then incubated with
167 GOT1 antibody-Magnetic Beads mixture overnight at 4°C. The immune

168 complexes were washed with IP Lysis Buffer for five times and subsequently
169 boiled with 2X sample buffer for 10 minutes, the GOT1-IP samples were then
170 resolved by SDS-PAGE. The endogenous acetylation level of GOT1 was
171 determined by western blotting using an anti-Acetylation antibody (CST,
172 9441S).

173

174 **Histology**

175 Pancreatic tissues were fixed with 4% paraformaldehyde, embedded in
176 paraffin and then analyzed with hematoxylin and eosin (H&E),
177 immunofluorescence, immunohistochemistry, or Alcian blue staining on 5µm
178 sections. For immunofluorescence, paraffin-embedded tissue slides were
179 deparaffinized by xylene and hydrated using decreasing ethanol gradients.
180 Next, tissue slides were probed with primary antibodies diluted in PBST with 5%
181 BSA at 4°C overnight, followed by incubation with 1:100 secondary antibodies
182 conjugated with Alexa Fluor® 488 donkey anti-rat IgG and Alexa Fluor® 594
183 donkey anti-rabbit IgG. After being mounted using Anti-fade Fluorescence
184 Mounting Media with DAPI, images were captured using an inverted fluorescent
185 microscope. Alcian blue staining was performed according to manufacturer's
186 instructions. In brief, the paraffin-embedded tissue sections were deparaffinized
187 by xylene, hydrated using gradient ethanol and then incubated at room
188 temperature for 30 minutes with Alcian Blue solution. The tissue sections were
189 washed with running tap water, followed by counterstaining with eosin.

190

191 **Immunohistochemistry**

192 For immunohistochemical analysis of SIRT5, Ki67 and Cleaved Caspase3,
193 antigen retrieval was performed by boiling the tissue slides in the Epitope
194 Retrieval Solution (pH 6). After blocking with 5% BSA solution containing 1%
195 goat serum, slides were incubated with indicated primary antibodies overnight
196 at 4°C. Next, the slides were incubated by VECTASTAIN® Elite® ABC HRP Kit
197 (PK-6100, VECTOR, USA) and ImmPACT® DAB Peroxidase (HRP) Substrate
198 (SK-4105, VECTOR, USA) according to the manufacturer's protocol. The
199 stained slides were scanned using Roche Ventana iScan HT System (Tissue
200 Science Facility Core, UNMC). The Ki67 positive staining cells were counted
201 from three random 20X fields in a section. For SIRT5 IHC score, two
202 pathologist-trained blinded observers evaluated the IHC results independently
203 according to an established semi-quantitative approach, which was evaluated
204 by both the staining intensity and the percentage of positive staining cells in
205 tumor cells. The staining intensity of the malignant cells was scored as 0, 1, 2,
206 or 3 for negative, weak, intermediate, and strong staining respectively. The
207 proportion represents the percentage of positively stained cells (0 = none, 1 =<
208 5%, 2 = 5 - 25%, 3 = 26 - 50%, 4 = 51 - 75%, 5 >= 75%). The overall protein
209 expression level in every IHC sample is given as a histoscore, which was

210 calculated by multiplying the proportion (0–5) and intensity scores (0–3). The
211 value of the histoscore ranges from 0 to 15, with a maximum of 15³. For the
212 survival analysis in Figure 1H-I, low SIRT5 expression is defined as SIRT5 IHC
213 histoscore < 7.5 and high SIRT5 expression is defined as SIRT5 IHC histoscore
214 ≥ 7.5.

215
216

217 **Plasmids**

218 The pcDNA3.1-hSIRT5-Flag, pcDNA3.1-hSIRT5 H158Y-HA plasmids were
219 kindly provided by Dr. Eric Verdin (Addgene plasmid # 13816). The catalytically
220 inactive mutant SIRT5 H158Y-Flag and pLX304-SIRT5 H158Y were generated
221 based on pcDNA3.1-hSIRT5-Flag and pLX304-SIRT5 plasmid using KOD-
222 Plus-Mutagenesis Kit (SMK-101, Toyobo, Japan). The human GOT1-HA
223 Lentiviral Vector was purchased from Applied Biological Materials Inc.
224 (LV791704). GOT1 mutant construct K276R, K290R, and K369R were
225 generated by PCR amplification using KOD-Plus-Mutagenesis Kit based on the
226 above GOT1-HA vector according to the manufacturer's protocol. The primers
227 used for plasmid construction are listed in Supplementary Table S4.

228

229 **Cell Growth and Clonogenic Assays**

230 For the cell growth assay, 1×10^5 PDAC cells were seeded in 6 cm culture
231 dishes (Corning, USA). These cells were trypsinized, stained with trypan blue
232 (Gibco, USA) and counted using BioRad TC20 automated cell counter at
233 indicated time points after inoculation. For the clonogenic assay, 200 PDAC
234 cells were seeded in six-well cell culture plates (Corning, USA), and cell culture
235 media was replaced every three days. Colonies were fixed with methanol and
236 then stained with 0.2% crystal violet in 80% methanol. The soft agar cell colony
237 formation assay was conducted according to the protocol of CytoSelect 96-Well
238 Cell Transformation Assay (Cell Biolabs, Inc.; San Diego, CA USA). In brief,
239 5,000 cells were suspended in 75 μ L 0.4% agar DMEM solution and seeded
240 over 50 μ L of bottom agar in 96-well plates. Images of colonies were captured
241 after 10 days using the Cytation 3 Cell Imaging Multi-Mode Reader (BioTek
242 Instruments, Inc.; Winooski, VT, USA). For 3D anchorage-free colony formation
243 assay, 5,000 cells were seeded in 200 μ L DMEM supplemented with 10% FBS
244 in 96-well ultra-low attachment microplate (7007; Corning, USA). Cell culture
245 media was refreshed every three days, and images of 3D colonies were
246 captured using Cytation 3 Cell Imaging Multi-Mode Reader. The volume of 3D
247 colonies was calculated using the formula: $\text{Volume} = 4/3\pi R^3$

248

249 **ROS Assay**

250 The intracellular ROS levels were measured as described previously⁴. In
251 brief, the oxidation-sensitive fluorescent dye 2',7'-dichlorofluorescein diacetate

252 (DCFDA) was used to detect the ROS level. The control and SIRT5 knockdown
253 PDAC cells were seeded in a clear-bottom black 96-well plate (3×10^4 cells/per
254 well). The cell culture medium was refreshed by the DMEM medium containing
255 20 μ M DCFDA. H_2O_2 combined with DCFDA was used as the positive control,
256 while 2',7'-Bis(2-carboxyethyl)-5(6)-carboxyfluorescein (CDCFDA) served as
257 the negative control and utilized for data normalization. All these cells were
258 incubated at 37°C for 30 min before testing. The cells were washed with 1X
259 PBS solution, and next the emission of DCFDA was detected using the BioTek
260 Cytation 3 plate reader (BioTek Instruments, Inc.; Winooski, VT, USA). The
261 DCFDA fluorescence signals were measured at the 495nm excitation
262 wavelength and 529nm emission wavelength.

263

264 **Enzyme Activity Assays**

265 The enzyme activities of GOT were measured using a Glutamate-
266 Oxaloacetate Transaminase Activity Assay Kit (MAK055, Sigma-Aldrich; St.
267 Louis, MO, USA) based on the manufacturer's protocol. In brief, 1×10^6 cells
268 were homogenized in 200 μ L ice-cold AST Assay Buffer. After removing the
269 insoluble material by centrifuging at 13000g for 10 minutes, the samples were
270 incubated at 37°C for 2 minutes while protected from light. The absorbance at
271 450 nm was monitored every five minutes using the Cytation 3 Cell Imaging
272 Multi-Mode Reader. To determine the GOT activity in MC3138-treated tumor
273 tissues, 50 mg tumor tissues from control and MC3138-treated groups were
274 ground into powder under with liquid nitrogen. Then the tumor tissue powder
275 was homogenized in 200 μ L of ice-cold AST Assay Buffer by vortex. Samples
276 were centrifuged at 13,000g for 10 minutes to remove the insoluble material.
277 20 μ L of samples were used for the GOT activity test as above. The enzyme
278 activity of GLS and GLUD1 were determined by the Glutaminase Assay Kit
279 (catalog #E-133, Biomedical Research Service Center; Buffalo, NY, USA) and
280 Glutamate Dehydrogenase Assay Kit (catalog #E-123, Biomedical Research
281 Service Center; Buffalo, NY, USA) respectively according to the manufacturer's
282 instructions. Briefly, 1×10^6 cells were homogenized and then mixed with 100
283 μ L ice-cold 1X cell lysis Solution. Then the lysate was incubated on ice for five
284 minutes with gentle agitation. After removing the insoluble material by
285 centrifuging at 14,000 rpm for five minutes, the supernatant was incubated at
286 37°C for one hour, protected from light. The optical density values at 492 nm
287 were measured by the Cytation 3 Cell Imaging Multi-Mode Reader. The
288 indicated enzyme activity was calculated using the above optical density value
289 data according to the manufacturer's instruction.

290

291 **Mass Spectrometric Metabolomics Analysis**

292 For metabolite extraction, PDAC cells were cultured in 6 cm cell culture
293 dishes (Corning, USA) and fresh cell culture medium was added two hours prior

294 to the metabolite extraction. Cells were washed twice with ice-cold PBS, and
295 then polar metabolites were extracted by adding cold 80% methanol/water (v/v,
296 -80°C). The lysates were centrifuged for 10 minutes at 13,500g. Next, the
297 supernatant was evaporated using the SpeedVac Vacuum Concentrator
298 (Thermo Fisher Scientific; Waltham, MA, USA). Lyophilized concentrates were
299 dissolved using equal volume LC-MS-grade water and then analyzed by liquid
300 chromatography tandem mass spectrometry (LC-MS/MS) using the selected
301 reaction monitoring (SRM) method ⁵. Peak areas were integrated using Skyline
302 software ⁶ and normalized by cell number from parallel plates and the internal
303 control. The normalized peak areas values were subjected to pathway
304 enrichment and relative quantification analyses using Metaboanalyst 3.0 ⁷. For
305 uniform ¹³C-labeled glutamine ([U-¹³C₅] glutamine) based flux analysis, PDAC
306 cells were grown to around 80% confluence in complete cell culture media.
307 Next, the complete medium was replaced by the glutamine/glucose-free DMEM
308 supplemented with 10% dialyzed FBS, 25 mM unlabeled glucose (Sigma-
309 Aldrich; St Louis, MO, USA), and 2 mM [U-¹³C₅] glutamine (Cambridge Isotope
310 Laboratories; Tewksbury, MA, USA) at indicated time point. Metabolites were
311 extracted and analyzed by LC-MS/MS analysis using SRM method.

312

313 **Lentivirus Transfection**

314 Stable short hairpin RNA (shRNA) targeting SIRT5, GOT1, and GOT2 were
315 obtained from Sigma-Aldrich. The plasmids overexpressing SIRT5 and the
316 corresponding empty-vector pLX304 were purchased from DNASU Plasmid
317 Repository (Arizona State University, Tempe, AZ, USA). CRISPR sgRNA
318 targeting control or different regions of GOT1 were purchased from Applied
319 Biological Materials Inc (Richmond, BC, Canada). Lentivirus was produced by
320 transfecting HEK293T cells with the desired plasmid and packaging constructs
321 using Turbofect. Cells were infected by the lentivirus with polybrene and then
322 selected with the indicated antibiotics. For CRISPR sgRNA-mediated knockout,
323 a single colony was isolated and propagated.

324

325 **Sirtuins Deacetylase Activity Assay**

326 Sirtuins deacetylase activity was measured using the SIRT1, SIRT3, and
327 SIRT5 Deacetylase Fluorimetric Activity Assay Kit (#ab156065, #ab156067,
328 #ab210074, Abcam) according to the manufacturer's guidelines. In brief, the
329 indicated sirtuin activators were co-incubated with Fluoro-Substrate Peptide,
330 NAD⁺, developer, and recombinant sirtuin enzymes at 37°C for 30 min. The
331 fluorescent intensity was detected using a BioTek Cytation 3 plate reader
332 (BioTek Instruments; Winooski, VT, USA) at 350 nm/450 nm (for SIRT1 and
333 SIRT3 activity assay) and 480 nm/530 nm (SIRT5 activity assay).

334

335 **Synthesis of MC3138**

336 The compound MC3138 (compound “7o” in previous literature) was
337 prepared in the Mai’s lab. The detailed synthetic procedure has been previously
338 described ⁸.

339

340 **Docking of MC3138 with SIRT5**

341 Sirt5 (PDB ID: 2B4Y) was retrieved from Protein Data Bank and MC3138
342 was prepared by downloading the 2D structure (PubChem CID 155524917) in
343 SDF format from Pubchem followed by conversion to 3D. The docking study
344 was carried out with AutoDock 4.2.6 (Scripps Research Institute). Visual
345 analysis of complex of MC3138 in the active centers of the Sirt5 (PDB ID: 2B4Y)
346 was performed using the Discovery Studio Visualizer (Figure 7a). The complex
347 showed a binding energy of -7.1 kcal/mol.

348

349 **MC3138 Pharmacokinetics**

350 For pharmacokinetics analysis of MC3138, C57BL/6J mice were intra-
351 peritoneally injected with a single dose of MC3138 [diluted in DMSO (1): corn
352 oil (9) solution, 200 mg/kg]. Mice were euthanized at indicated time points (0.5
353 h, 1 h, 3 h, 7 h, 12 h, 24 h, 48 h) to collect plasma and organs with n=4 for each
354 time point. For MC3138 extraction, 50 μ L plasma was mixed with 2 mL acetone
355 and vortexed thoroughly for 3 min. Samples were then centrifuged at 3500 rpm
356 for 10 min. The supernatant was transferred into a new tube and evaporated
357 using a SpeedVac. The dried extract was reconstituted in 50 μ L methanol and
358 diluted with water into a final composition of 10% methanol, then purified by
359 strata-x polymeric reverse phase columns (88-S100-UBJ Phenomenex), using
360 an activation procedure consisting of consecutive washes with 3 mL of 100%
361 methanol followed by 3 mL of water. After the samples were loaded into the
362 column, 2 mL 50% methanol was used to wash out the contamination, and 2.5
363 mL methanol was then used to elute the drug. The eluent was transferred into
364 autoinjector sample vials for LC-MS/MS analysis. LC-MS/MS analysis was
365 performed with Waters ACQUITY UPLC systems connected to a Xevo TQ-S
366 mass spectrometry using Multiple Reaction Monitoring (MRM) transitions
367 436.1888->104.8490 and 436.1888->390.1448. Chromatographic separation
368 was performed on a Waters UPLC BEH C18 column (2.1 \times 100 mm, 1.7 μ m)
369 with a gradient of solvents A (methanol) and solvents B (water). The gradient
370 was as follows: 0 min, 50% A, 10 min, 80% A, 15 min, 80% A, 16 min 50% A,
371 20 min, and 50% A.

372 To determine the concentration of MC3138 in tumor tissues, MC3138 was
373 extracted from 50 mg tumor tissues from MC3138-treated and control groups.
374 In brief, tumor tissues were ground into powder while cooling in liquid nitrogen.
375 Then the powder was mixed with 2 mL acetone and vortexed thoroughly for 3
376 min. Samples were then centrifuged at 3500 rpm for 10 min. The supernatant
377 was transferred into a new tube and evaporated using a SpeedVac. The dried

378 extract was reconstituted in 50 μ L methanol and diluted with water into a final
379 composition of 10% methanol, then purified by strata-x polymeric reverse
380 phase columns (88-S100-UBJ Phenomenex), using an activation procedure
381 consisting of consecutive washes with 3 mL of 100% methanol followed by 3
382 mL of water. After the samples were loaded into the column, 2 mL 50%
383 methanol was used to wash out the contamination, and 3 mL methanol was
384 then used to elute the drug. The eluent was transferred into autoinjector sample
385 vials for LC-MS/MS analysis. LC-MS/MS analysis was performed with Waters
386 ACQUITY UPLC systems connected to a Xevo TQ-S mass spectrometry using
387 Multiple Reaction Monitoring (MRM) transitions 436.1888->104.8490 and
388 436.1888->390.1448. Chromatographic separation was performed on a Waters
389 UPLC BEH C18 column (2.1 \times 100 mm, 1.7 μ m) with a gradient of solvents A
390 (methanol) and solvents B (water). The gradient was as follows: 0 min, 50% A,
391 10 min, 80% A, 15 min, 80% A, 16 min 50% A, 20 min, and 50% A.

392

393 **Statistical Analysis**

394 All data are shown as mean \pm standard deviation (SD) from at least three
395 independent experiments except when indicated. Log-rank tests and Kaplan-
396 Meier method were used to perform survival analysis. The χ^2 test or Fisher's
397 Exact test was used to analyze the qualitative variables of clinicopathological
398 data. Univariate and multivariate Cox proportional hazards regression were
399 used to evaluate the prognostic factors in the PDAC patients. The statistical
400 analyses between the two groups were performed by two-tailed Student's t-test.
401 The statistical difference between multiple groups was conducted using one-
402 way ANOVA with Bonferroni's post hoc analysis or Tukey's post hoc analysis.
403 The correlation analysis was conducted using the Pearson's correlation test. All
404 statistical analysis was performed using GraphPad Prism (Version 6) and
405 SPSS 22.0. Statistical analyses were two-tailed and used an alpha of 0.05 for
406 these tests. All quantitative *in vitro* experiments were repeated at least three
407 times in triplicates.

408

409 **Supplementary References**

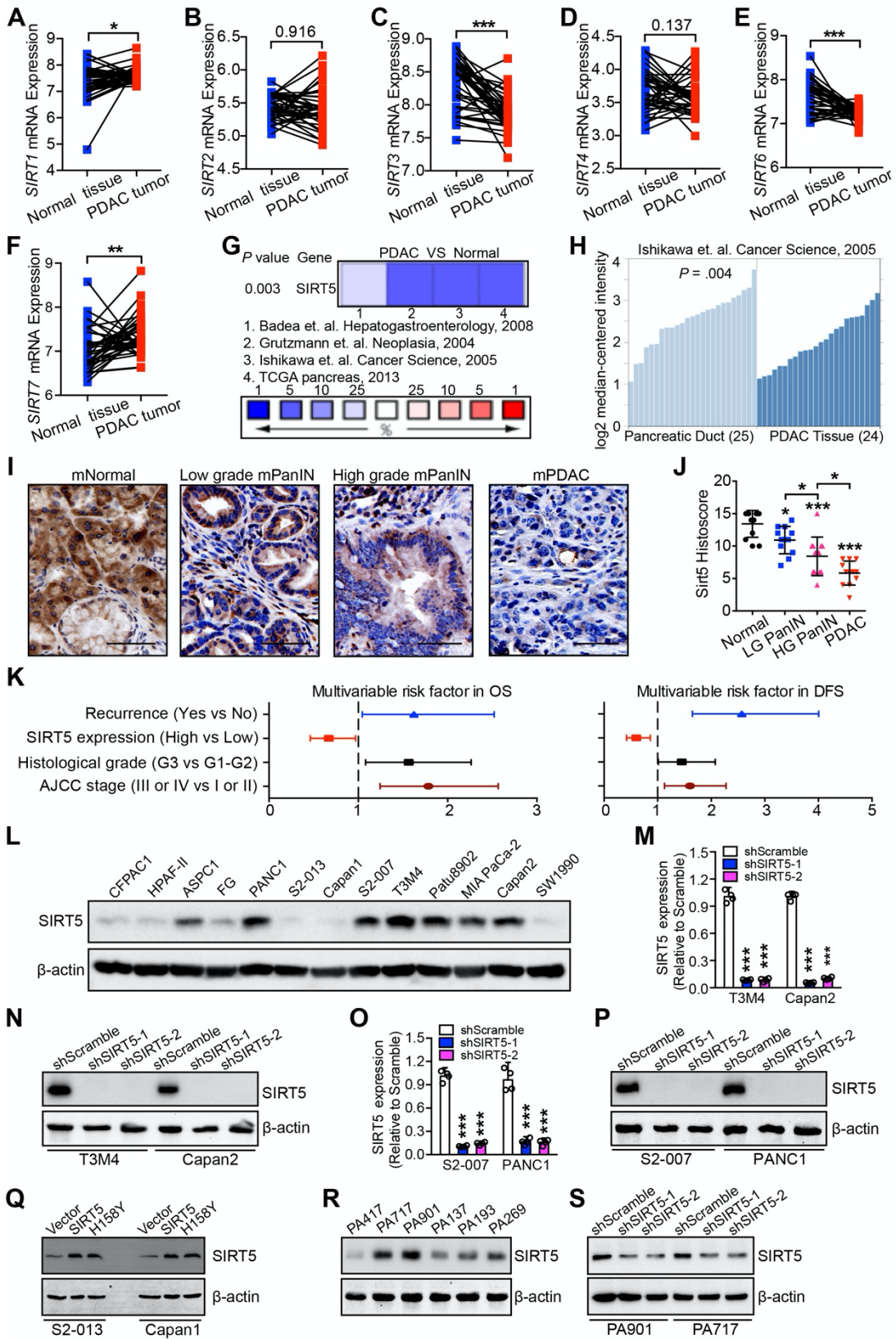
- 410 1. **Boj SF, Hwang CI, Baker LA**, et al. Organoid models of human and
411 mouse ductal pancreatic cancer. *Cell* 2015;160:324-38.
- 412 2. Schmittgen TD, Livak KJ. Analyzing real-time PCR data by the
413 comparative C(T) method. *Nat Protoc* 2008;3:1101-8.
- 414 3. Chaika NV, Yu F, Purohit V, et al. Differential expression of metabolic
415 genes in tumor and stromal components of primary and metastatic loci
416 in pancreatic adenocarcinoma. *PLoS One* 2012;7:e32996.
- 417 4. Abrego J, Gunda V, Vernucci E, et al. GOT1-mediated anaplerotic
418 glutamine metabolism regulates chronic acidosis stress in pancreatic
419 cancer cells. *Cancer Lett* 2017;400:37-46.

- 420 5. Gunda V, Yu F, Singh PK. Validation of Metabolic Alterations in
421 Microscale Cell Culture Lysates Using Hydrophilic Interaction Liquid
422 Chromatography (HILIC)-Tandem Mass Spectrometry-Based
423 Metabolomics. PLoS One 2016;11:e0154416.
- 424 6. MacLean B, Tomazela DM, Shulman N, et al. Skyline: an open source
425 document editor for creating and analyzing targeted proteomics
426 experiments. Bioinformatics 2010;26:966-8.
- 427 7. Xia J, Sinelnikov IV, Han B, et al. MetaboAnalyst 3.0--making
428 metabolomics more meaningful. Nucleic Acids Res 2015;43:W251-7.
- 429 8. Valente S, Mellini P, Spallotta F, et al. 1,4-Dihydropyridines Active on
430 the SIRT1/AMPK Pathway Ameliorate Skin Repair and Mitochondrial
431 Function and Exhibit Inhibition of Proliferation in Cancer Cells. J Med
432 Chem 2016;59:1471-91.

433 Author names in bold designate shared co-first authorship.

434

435



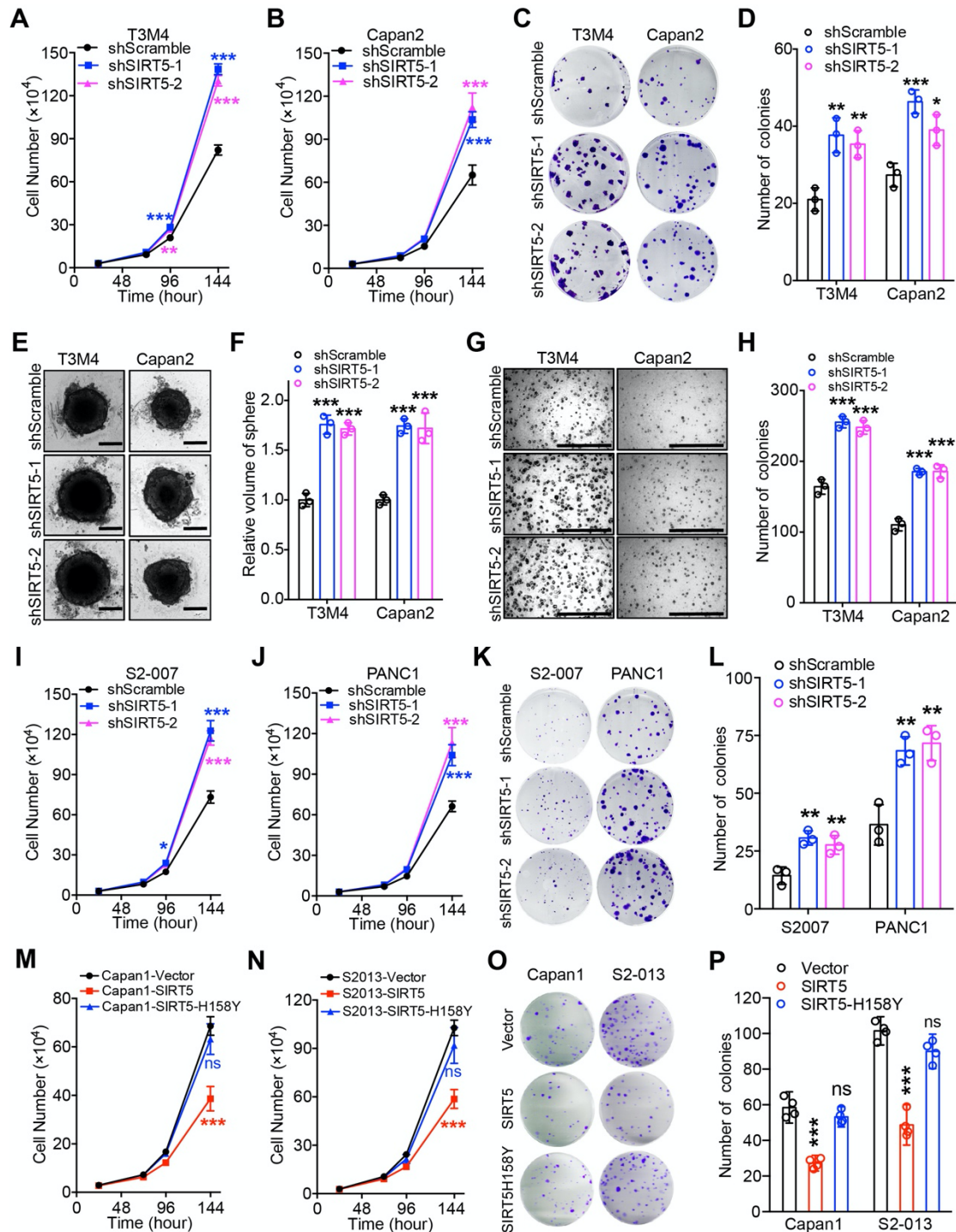
437

438

439

Figure S1. SIRT5 downregulation in PDAC correlates with disease progression, poor survival outcomes, and enhanced tumor cell growth.

440 (A-F). The mRNA levels of *SIRT1-7* in pancreatic cancer tissues and the paired
441 adjacent normal tissues from GEO database (GDS4103, n = 39).
442 (G-H). *SIRT5* mRNA is downregulated in pancreatic cancer tissues among
443 various cohorts from the Oncomine database (<https://www.oncomine.org>). The
444 representative scatter plot of *SIRT5* mRNA level from the Ishikawa cohort (H).
445 (I-J). IHC staining (I) and quantification (J) for *SIRT5* expression in normal
446 acinar cells from control mice and low-grade (LG) PanINs, high-grade (HG)
447 PanINs, and pancreatic tumors from KPC mice. Scale bar represents 100 μ m.
448 (K). Multivariate regression analysis of the overall survival and disease-free
449 survival in PDAC patient cohort from Shanghai Outdo Biotech Tissue Bank
450 (Bars indicate 95% confidence intervals).
451 (L). Immunoblotting for *SIRT5* expression in thirteen pancreatic cancer cell lines.
452 (M-P). qRT-PCR and immunoblotting for *SIRT5* expression in control and
453 *SIRT5*-knockdown PDAC cells.
454 (Q). Immunoblotting for *SIRT5* expression in control, *SIRT5*-overexpressing
455 and *SIRT5*H158Y-overexpressing PDAC cells.
456 (R). Immunoblotting for *SIRT5* expression in six human PDAC organoids.
457 (S). Immunoblotting of *SIRT5* expression levels in the control and *SIRT5*-
458 knockdown PDAC organoids.
459 For all *in vitro* studies $n \geq 3$. The data are represented as mean \pm SD. The
460 statistics is calculated by paired Student's t-test (A-F). The cohorts were
461 compared with the control group by one-way ANOVA with Bonferroni's post hoc
462 analysis (M, O) or compared with every other group by one-way ANOVA with
463 Tukey's post hoc analysis (J), * $P < .05$, ** $P < .01$, and *** $P < .001$.
464



465

466

Figure S2. SIRT5 inhibits pancreatic cancer cell growth *in vitro*.

467

(A-B). The cell growth curve of control and *SIRT5*-knockdown T3M4 and Capan2 PDAC cells.

468

(C-D). Representative images and quantitation of colony formation assay in control and *SIRT5*-knockdown T3M4 and Capan2 PDAC cells.

470

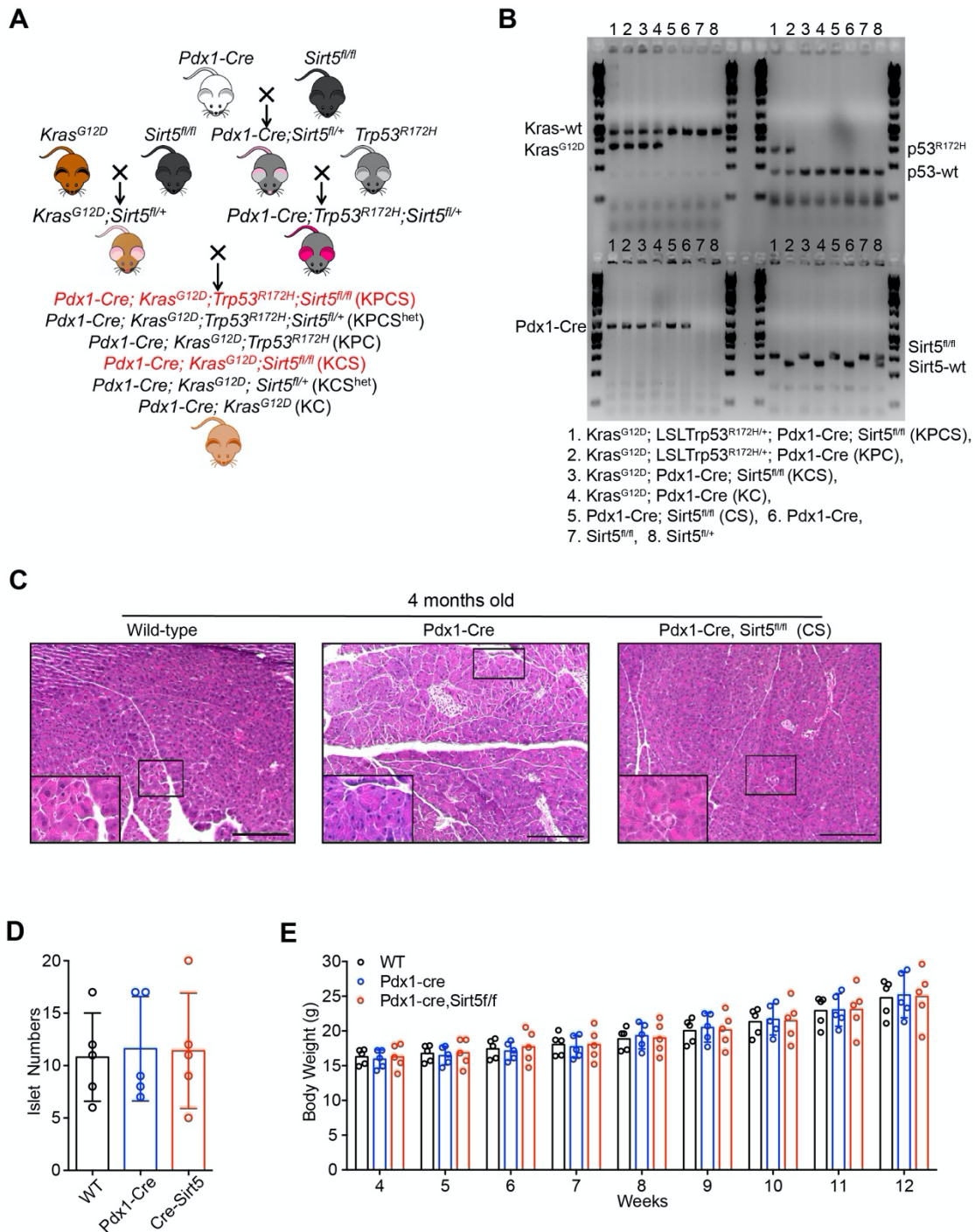
(E-F). Sphere formation assay with control and *SIRT5*-knockdown T3M4 and

471

Capan2 PDAC cells that were grown in 96-well low attachment plates for 15

472

473 days. Images were captured by Cytation 3 and sphere volume was calculated
474 by $V=4*\pi r^3/3$. Scale bar represents 300 μm .
475 (G-H). Representative images and quantitation of colonies in soft agar colony
476 formation assays for control and *SIRT5*-knockdown T3M4 and Capan2 PDAC
477 cells. Scale bar represents 1000 μm .
478 (I-J). Growth rates of control and *SIRT5*-knockdown PANC1 and S2-007 PDAC
479 cells.
480 (K-L). Representative images and quantitation of the colony formation assay in
481 control and *SIRT5*-knockdown PANC1 and S2-007 PDAC cells.
482 (M-N). Growth rates of control, *SIRT5*-overexpressing and SIRT5H158Y-over
483 expressing cells (Capan1 and S2-013).
484 (O-P). Representative images and quantitation of the colony formation assay
485 in control, *SIRT5*-overexpressing and SIRT5H158Y-overexpressing cells
486 (Capan1 and S2-013).
487 For all *in vitro* studies $n \geq 3$. The data are represented as mean \pm SD. The
488 cohorts were compared with the control group by one-way ANOVA with
489 Bonferroni's post hoc analysis (D, F, H, L, P). Cohorts were compared with the
490 control group by two-way ANOVA with Bonferroni's post hoc analysis (A, B, I,
491 J, M, N), * $P < .05$, ** $P < .01$, and *** $P < .001$.
492



493

494 **Figure S3.** SIRT5 deficiency in murine pancreas does not display distinct
 495 abnormalities.

496 All panels shown are age-matched wild-type C57 mice, *Pdx1-Cre* (Cre), and
 497 *Pdx1-Cre, Sirt5^{fl/fl}* (CS) littermate mice (n = 5, each group).

498 (A). *LSL-Kras^{G12D}*, *LSL-Trp53^{R172H/+}*, and *Pdx1-Cre* mice were crossed with
 499 *Sirt5^{fl/fl}* mice to obtain mice with *Kras^{G12D}; Sirt5^{fl/+}* (KS^{het}) and *LSL-Trp53^{R172H/+};*
 500 *Pdx1-Cre; Sirt5^{fl/fl}* (PCS^{het}) genotypes. Intercrossing of the KS^{het} and PCS^{het}
 501 mice generated *LSL-Kras^{G12D}; LSL-Trp53^{R172H/+}; Pdx1-Cre; Sirt5^{fl/fl}* (KPCS) and
 502 *LSL-Kras^{G12D}; LSL-Trp53^{R172H/+}; Pdx1-Cre* (KPC) mice.

503 (B). Representative images depicting the genotyping results of tissues
504 extracted from KPCS (lane 1), KPC (lanes 2), KCS (lane 3), KC (lane 4), CS
505 (lane 5), *Pdx1-Cre* (lane 6), *Sirt5^{fl/fl}* (lane 7), and *Sirt5^{fl/+}* (lane 8) mice.

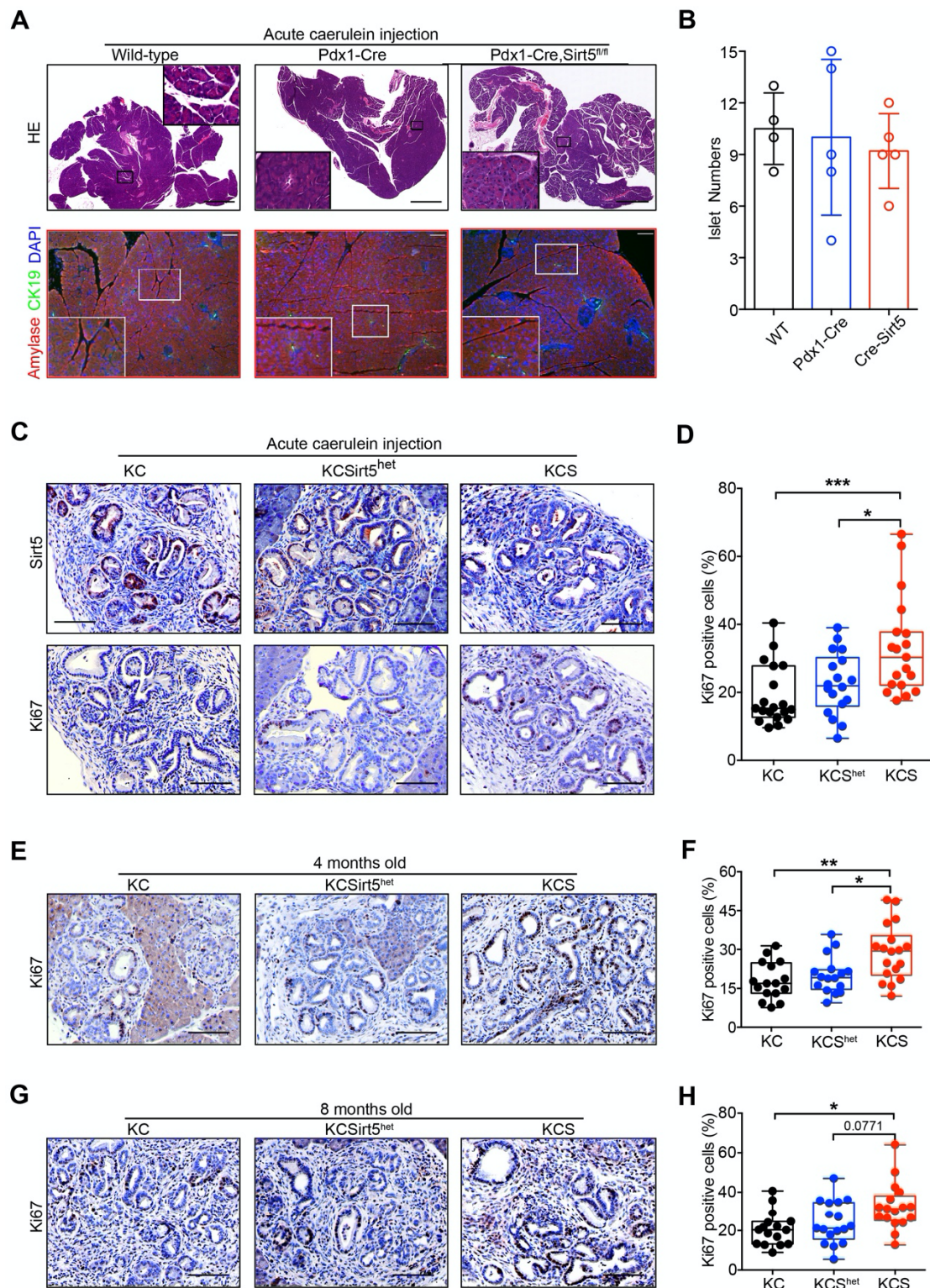
506 (C). Representative image of H&E stained pancreatic tissues from mice of
507 indicated genotypes at 16 weeks of age. Scale bar is 200 μ m.

508 (D). Quantitation of the islet numbers in 16-week-old wild-type, *Pdx1-Cre*, and
509 CS mice.

510 (E). Body weight in age-matched wild-type, *Pdx1-Cre*, and CS mice from age 4
511 to 16 weeks.

512 The data are represented as mean \pm SD. The cohorts were compared with the
513 wild type group by one-way ANOVA with Bonferroni's post hoc analysis (D).
514 Cohorts were compared with every other group by two-way ANOVA with
515 Tukey's post hoc analysis (E). Differences between each group (D-E) are not
516 significant.

517

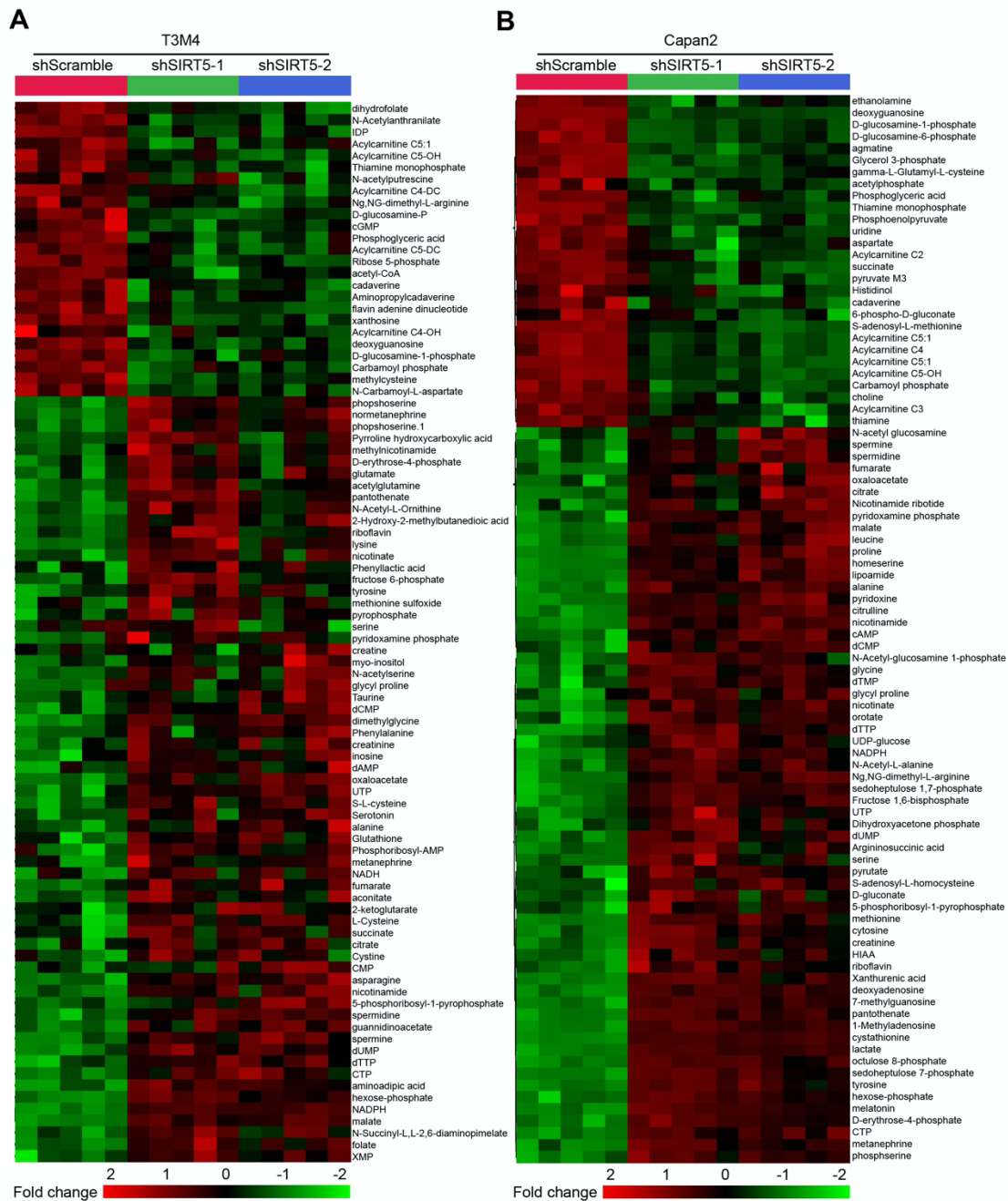


518

519 **Figure S4.** Sirt5 deficiency accelerates acinar-to-ductal metaplasia, PanIN
 520 formation, and PDAC progression cooperated with oncogenic mutations.

521 (A). Representative image of H&E staining and CK19/Amylase immunofluorescence staining of pancreatic tissue from the indicated genotype mice receiving
 522 two-days caerulein-injection. Scale bars: H&E 2000 μ m, immunofluorescence
 523 100 μ m.

525 (B). Statistical analysis of the islet number in the age-matched wild-type, *Pdx1-*
526 *Cre*, and CS mice receiving two-days caerulein-injection.
527 (C). IHC staining images of SIRT5 and Ki67 in pancreatic tissue from caerulein-
528 injected KC, KCS^{het}, and KCS mice. Scale bars are 100 μm.
529 (D). Quantification of Ki67 positive cells in pancreatic tissue from caerulein-
530 injected KC, KCS^{het}, and KCS mice.
531 (E-F). IHC staining and quantification of Ki67 positive cells in pancreatic tissue
532 from 4-month-old KC, KCS^{het}, and KCS mice. Scale bars are 100 μm.
533 (G-H). IHC staining and quantification of Ki67 positive cells in pancreatic tissue
534 from 8-month-old KC, KCS^{het}, and KCS mice. Scale bars are 100 μm.
535 The data are represented as mean ± SD. The cohorts were compared with
536 every other group by one-way ANOVA with Tukey's post hoc analysis (B, D, F,
537 H), **P*<.05, ***P*<.01, and ****P*<.001.
538



539

540

Figure S5 related to Figure 4. SIRT5 suppresses glutamine and glutathione metabolism, and regulates cellular redox homeostasis.

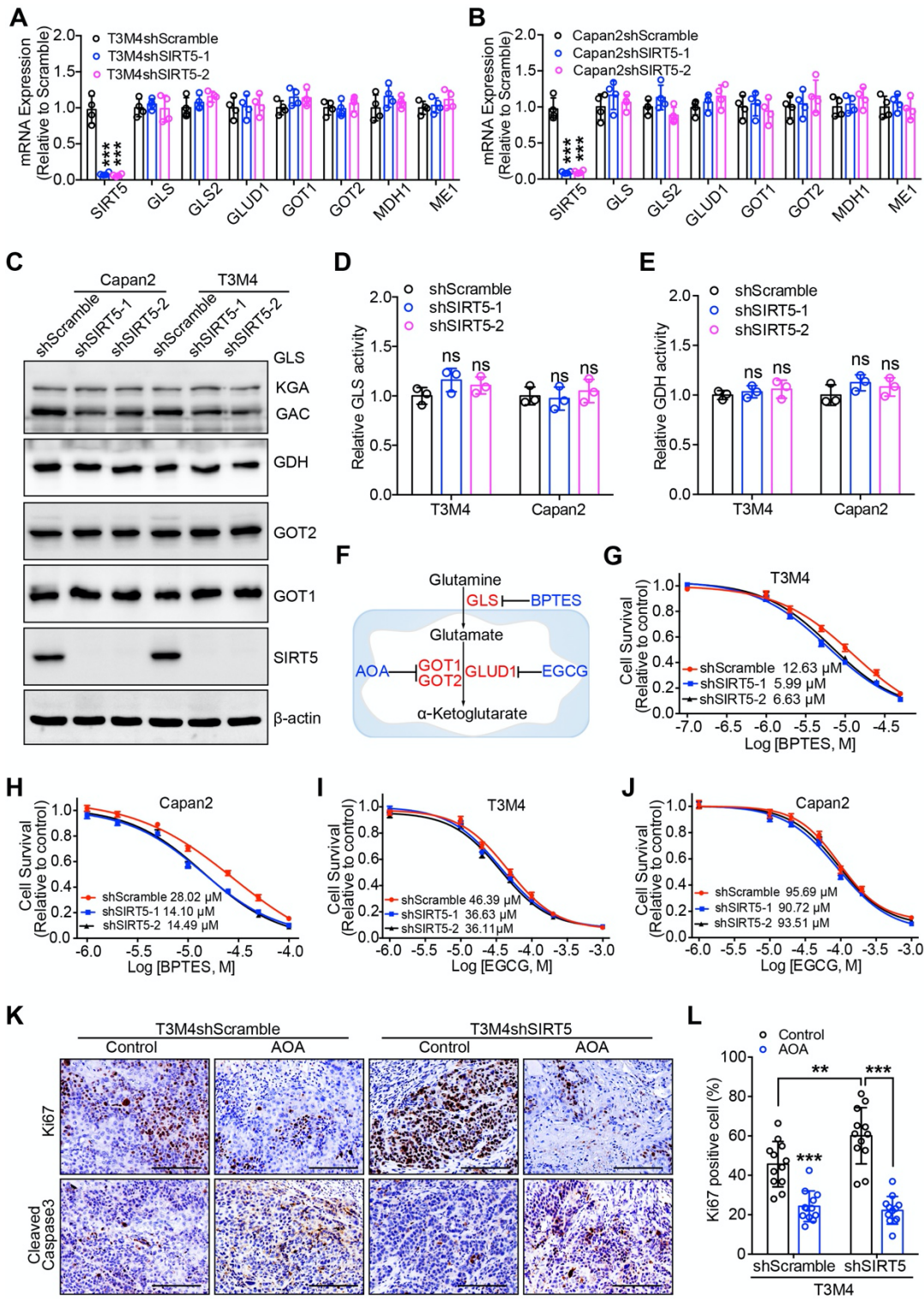
541

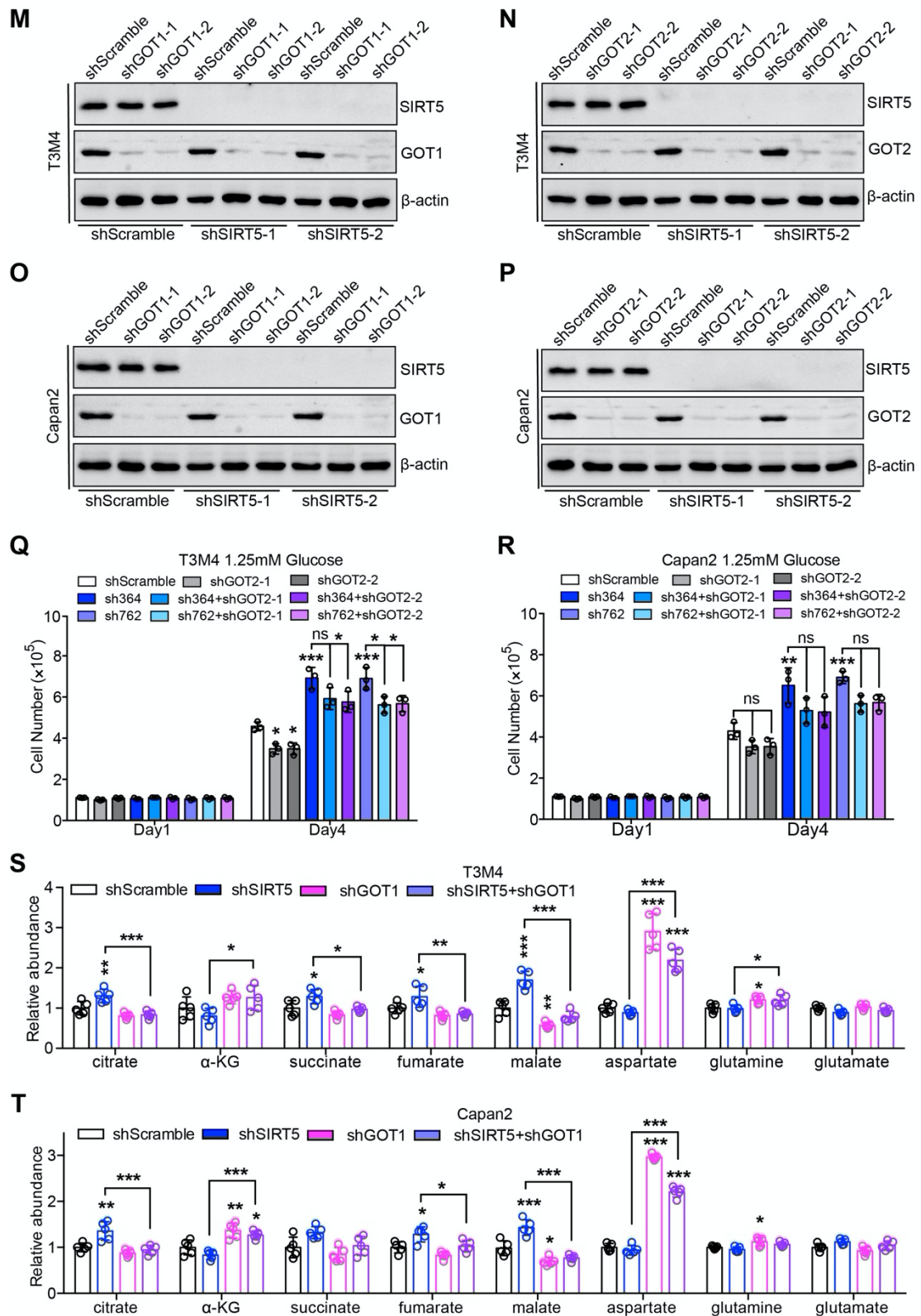
(A-B). The heatmap of significantly deregulated metabolites between control and *SIRT5*-knockdown PDAC cells (n= 5 samples for each group).

542

543

544





546

547 **Figure S6.** SIRT5 inhibits glutamine and glutathione metabolism by decreasing
 548 GOT1 enzyme activity.

549 (A-B). The mRNA levels of enzymes involved in glutamine and glutathione
 550 metabolism in control and *SIRT5*-knockdown PDAC T3M4 and Capan2 cells.

551 (C). The protein levels of enzymes involved in glutamine and glutathione
552 metabolism from control and *SIRT5*-knockdown PDAC cells.

553 (D). The GLS enzyme activity was determined in T3M4 and Capan2 *SIRT5*-
554 knockdown cells.

555 (E). The GDH (GLUD1) enzyme activity was determined in T3M4 and Capan2
556 *SIRT5*-knockdown cells.

557 (F). A schematic depiction of the key enzymes in glutamine metabolism and the
558 corresponding inhibitors. Bis-2-(5-phenylacetamido-1,3,4-thiadiazol-2-yl) ethyl
559 sulfide (BPTES), epigallocatechin gallate (EGCG), and aminooxyacetate
560 (AOA).

561 (G-H). Relative cell survival of control and *SIRT5*-knockdown cells treated with
562 GLS inhibitor BPTES. Data are presented relative to the respective untreated
563 control and *SIRT5*-knockdown cells.

564 (I-J). Relative cell survival of control and *SIRT5*-knockdown cells treated with
565 GLUD1 inhibitor EGCG. Data are presented relative to the respective untreated
566 control and *SIRT5*-knockdown cells.

567 (K-L). Ki67 IHC staining (K) and quantitation (L) in tumor sections from
568 orthotopically implanted scrambled control and *SIRT5*-knockdown cells treated
569 with saline control or AOA. Scale bars are 100 μ m.

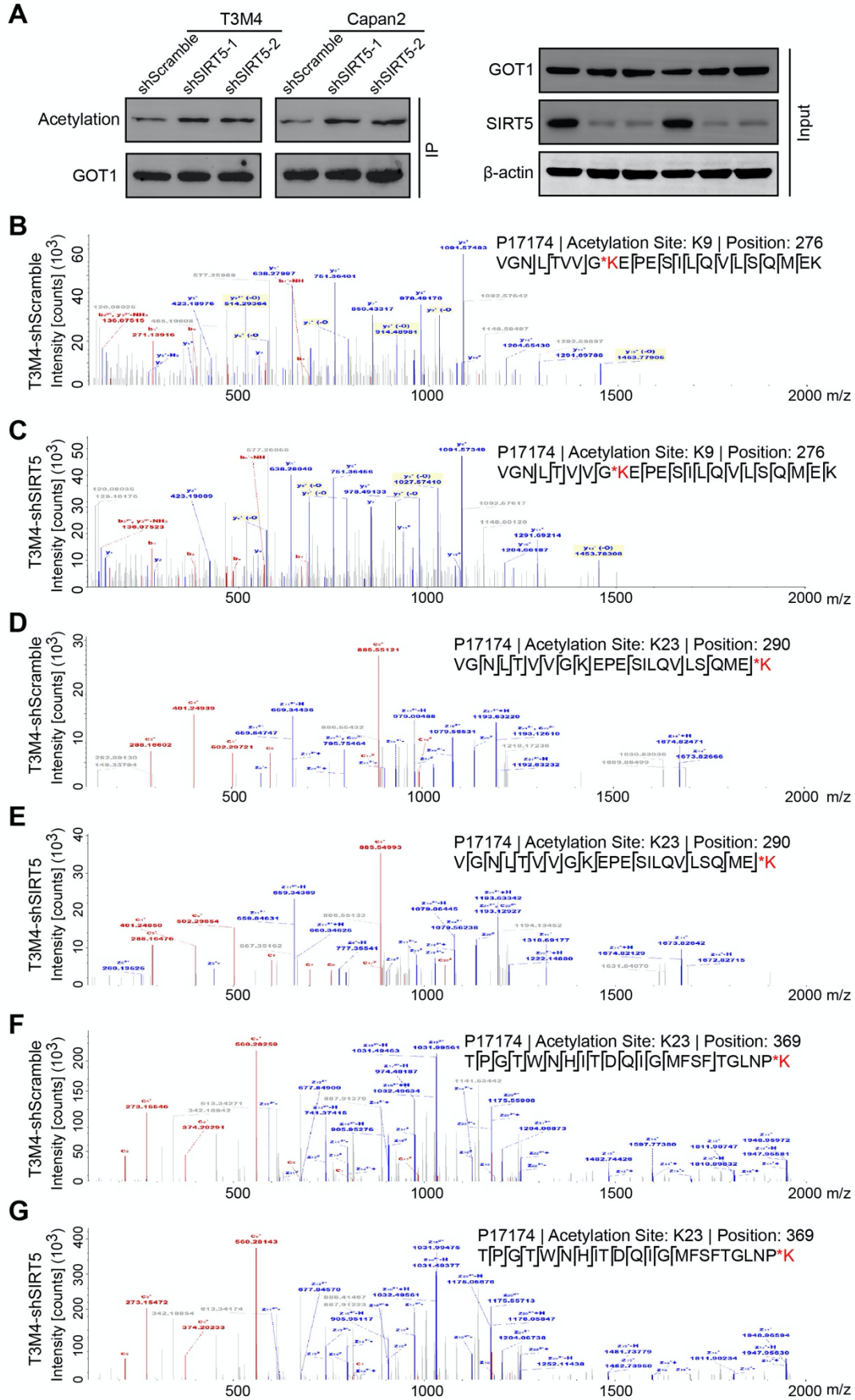
570 (M-P). Western blotting to confirm *GOT1* and *GOT2* knockdown efficiency in
571 scrambled control and *SIRT5*-knockdown cells.

572 (Q-R). Cell growth of scrambled control and *SIRT5*-knockdown cells
573 transfected with scrambled control or *GOT2* shRNA under low glucose
574 conditions (1.25 mM). Experiment for scrambled control and *SIRT5*-knockdown
575 cells transfected with *GOT1* or *GOT2* shRNA were set up together.

576 (S-T). Relative levels of metabolites in glutamine and glutathione metabolism
577 pathways from scrambled control and *SIRT5*-knockdown cells transfected with
578 scrambled control or *GOT1* shRNA.

579 For all *in vitro* studies $n \geq 3$. The data are represented as mean \pm SD. Cohorts
580 were compared with the control group by one-way ANOVA with Bonferroni's
581 post hoc analysis (A, B, D, E) or compared with every other group by one-way
582 ANOVA with Tukey's post hoc analysis (L, Q-T), * $P < .05$, ** $P < .01$, and
583 *** $P < .001$.

584

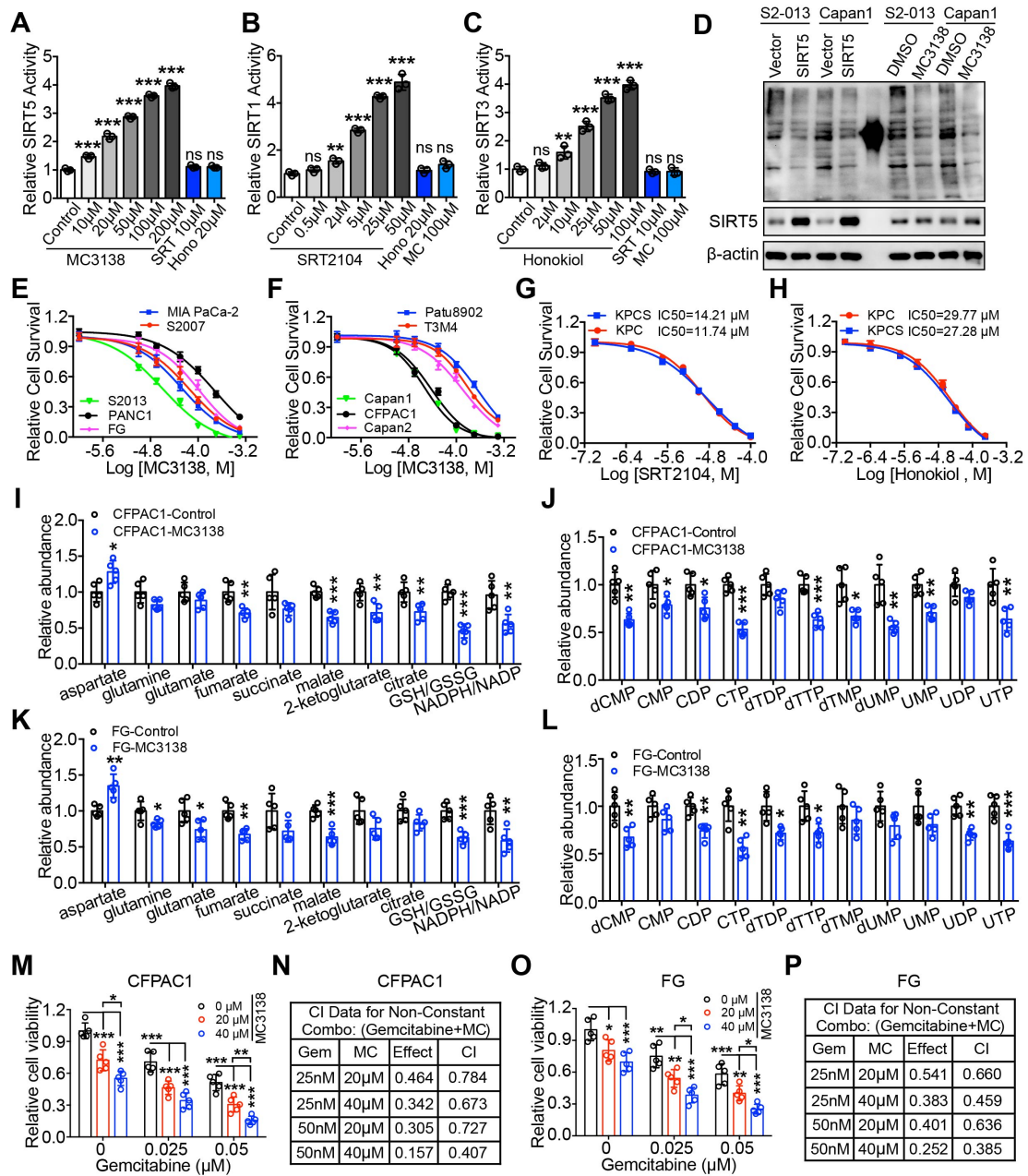


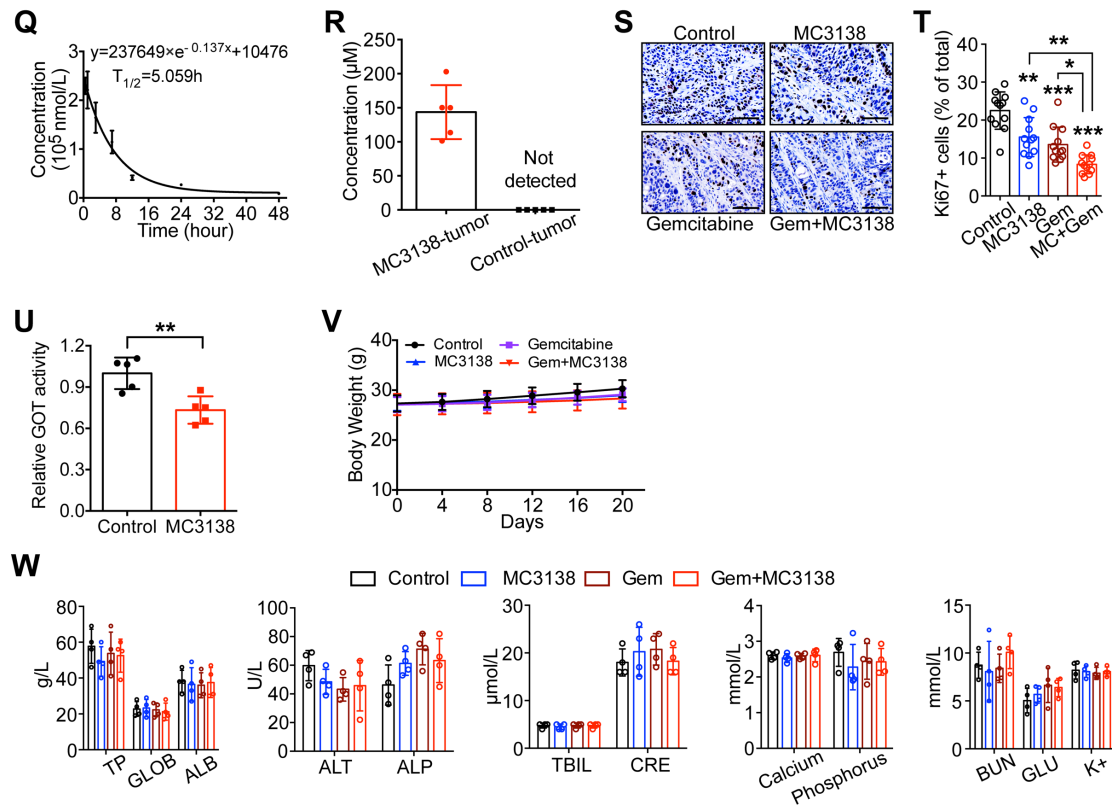
586 **Figure S7.** SIRT5 inhibits GOT1 enzymatic activity by catalyzing its lysine
587 deacetylation.

588 (A). Endogenous GOT1 protein was immunoprecipitated from control and
589 *SIRT5*-knockdown T3M4/Capan2 cells. The lysine acetylation level of GOT1
590 was determined by western blotting. Input protein levels are shown on the right.

591 (B-G). Mass spectra demonstrating lysine acetylation sites in exogenously
592 expressed GOT1 protein immunoprecipitated from scrambled control and
593 *SIRT5*-knockdown T3M4 cells. The specific lysine acetylation sites were
594 identified by the liquid chromatography-tandem mass spectrometry. The
595 identified acetylated peptide ions in GOT1 protein are indicated.

596





598

599 **Figure S8.** SIRT5 activator MC3138 exhibits anti-tumor effects and synergism
600 with gemcitabine in human PDAC cells, organoids, and PDX models.

601 (A). Increased SIRT5 deacetylase activity by MC3138. SIRT5 deacetylase
602 activity was measured under different concentrations of MC3138 using SIRT5
603 Deacetylase Fluorometric Assay Kit. The selective SIRT1 activator SRT2104
604 (SRT) and SIRT3 activator Honokiol (Hono) were used as negative controls.

605 (B-C). SIRT5 activator MC3138 does not increase SIRT1 and SIRT3
606 deacetylase activities. SIRT1 and SIRT3 deacetylase activities were detected
607 using SIRT1 and SIRT3 Deacetylase Fluorometric Assay Kits, respectively.
608 The selective SIRT1 activator SRT2104 and SIRT3 activator Honokiol were
609 used as positive controls.

610 (D). Immunoblotting to show the lysine acetylation level in control or *SIRT5*-
611 overexpressing PDAC cells and PDAC cells treated with DMSO solvent control
612 or 10 μ M SIRT5 activator MC3138 for 24 h.

613 (E-F). Relative cell survival of ten PDAC cell lines treated with different doses
614 of MC3138.

615 (G-H). Relative cell survival of KPC cell line and *SIRT5*-knockout KPC cell line
616 (KPCS) treated with different doses of SIRT1 activator SRT2104 and SIRT3
617 activator Honokiol.

618 (I-L). Bar charts depicting the relative levels of metabolites in glutamine,
619 glutathione and pyrimidine metabolism pathways in CFPAC1 and FG cells
620 treated with MC3138 (CFPAC1: 20 μ M; FG: 50 μ M) for 24 h.

621 (M, O). Cell viability of CFPAC1 (M) and FG (O) cells treated with the indicated
622 concentrations of gemcitabine and MC3138 for 72 h.
623 (N, P). Combination index (CI) of gemcitabine and MC3138 at indicated
624 concentrations was calculated using Compusyn software.
625 (Q). MC3138 Pharmacokinetics: The plasma concentration-time curve of
626 MC3138 after intraperitoneal injection of a single dose of MC3138 (200 mg/kg)
627 (n = 4).
628 (R). The concentration of MC3138 in tumor tissues from MC3138-treated
629 PA137 PDX tumors.
630 (S-W). Effect of MC3138 (MC) combined with Gemcitabine (Gem) on human
631 PDX tumors. IHC staining of Ki67 (S) and quantitation (T). The relative GOT
632 activity of control and MC3138-treated PA137 PDX tumors (U). The body
633 weights of mice from each group at indicated time points (V). The blood
634 biochemistry indices test results of mice from indicated groups by automatic
635 biochemical analyzer (W). Scale bars are 100 μ m.
636 For all *in vitro* studies $n \geq 3$. The data are represented as mean \pm SD. The
637 cohorts were compared with the control group by one-way ANOVA with
638 Bonferroni's post hoc analysis (A, B, C) or compared with every other group by
639 one-way ANOVA with Tukey's post hoc analysis (M, O, T, W). Cohorts were
640 compared with every other group by two-way ANOVA with Tukey's post hoc
641 analysis (V). The statistics was calculated by Student's t-test (I, J, K, L, R, U),
642 * $P < .05$, ** $P < .01$, and *** $P < .001$.
643

644 **Table S1. Correlation between Expression of SIRT5 and**
645 **Clinicopathological Features in PDAC Patients from Figure 1.**
646

Variables	Low SIRT5	High SIRT5	<i>p</i> value
Numbers	73	70	
Gender			0.161
Male	49 (67.1)	39 (55.7)	
Female	24 (32.9)	31 (44.3)	
Median age			0.801
<62 years	37 (50.7)	34 (48.6)	
≥62 years	36 (49.3)	36 (51.4)	
pT stage			0.160
T1-T2	44 (60.3)	50 (71.4)	
T3-T4	29 (39.7)	20 (28.6)	
pN stage			0.145
N0	36 (49.3)	43 (61.4)	
N1-N2	37 (50.7)	27 (38.6)	
pM stage ^a			0.962
M0	71 (97.3)	67 (95.7)	
M1	2 (2.7)	3 (4.3)	
TNM stage			0.148
I- II	35 (47.9)	42 (60.0)	
III- IV	38 (52.1)	28 (40.0)	
Histological grade ^b			0.659
G1	7 (9.6)	11 (15.7)	
G2	40 (54.8)	34 (48.6)	
G3	26 (35.6)	25 (35.7)	
Tumor size (cm)			0.765
≤4	42 (57.5)	42 (60.0)	
>4	31 (42.5)	28 (40.0)	
Recurrence			0.033
YES	55 (75.3)	41 (58.6)	
NO	18 (24.7)	29 (41.4)	
CEA (ng/mL)			0.339
<5	38 (52.1)	42 (60.0)	
≥5	35 (47.9)	28 (40.0)	
CA199 (U/mL)			0.783
<37	39 (53.4)	39 (55.7)	
≥37	34 (46.6)	31 (44.3)	
Location			0.016
head	45 (61.6)	29 (41.4)	
body/tail	28 (38.4)	41 (58.6)	

Neural Invasion			0.923
No	38 (52.1)	37 (52.9)	
Yes	35 (47.9)	33 (47.1)	
Chemotherapy			0.771
No	32 (43.8)	29 (41.4)	
Yes	41 (56.2)	41 (58.6)	
Chemotherapy (Yes)			0.888
Gemcitabine	16 (39.0)	13 (31.7)	
Gemcitabine + Capecitabine	7 (17.1)	9 (22.0)	
Gemcitabine + nab- paclitaxel	12 (29.3)	12 (29.3)	
Gemcitabine + Tegafur	6 (14.6)	7 (17.1)	

647 Note: All data are shown as numbers and percentages--numbers (percentage%). Chi-square Analysis
648 was used in these data.

649 a: The Yate's correction for continuity was used in data of this group.

650 b: The Kruskal Wallis Test was used in data of this group.

651

652

653 **Table S2. Univariate and Multivariate Analysis for the Prognostic Factors**
654 **of Overall Survival in PDAC Patients from Figure 1.**

655

Variables	Univariate		Multivariate	
	Analysis	P value	Analysis	P value
	HR (95% CI)		HR (95% CI)	
Gender (male versus female)	1.529 (1.049-2.230)	0.027	1.415 (0.953-2.099)	0.085
Age (≥62 years vs <62 years)	1.246 (0.871-1.782)	0.229		
pT status (T3 or T4 vs T1 or T2)	0.857 (0.587-1.252)	0.425		
pN status (N1-2 vs N0)	1.753 (1.222-2.515)	0.002	1.116 (0.390-3.196)	0.838
pM status (M1 vs M0)	1.562 (0.636-3.840)	0.331		
AJCC stage (III or IV vs I or II)	1.793 (1.250-2.572)	0.002	1.786 (1.243-2.568)	0.002
Histological grade (G3 vs G1 or G2)	1.558 (1.079-2.250)	0.018	1.565 (1.082-2.265)	0.018
Tumor size (≤4 cm vs >4 cm)	0.840 (0.584-1.207)	0.345	-	-
Recurrence (Yes vs No)	1.786 (1.167-2.734)	0.008	1.623 (1.045-2.522)	0.031
CEA (≥5 ng/mL vs <5ng/mL)	0.973 (0.681-1.390)	0.881		
CA199 (≥37 U/mL vs <37U/mL)	1.237 (0.863-1.771)	0.247	-	-
Location (Head vs Body/Tail)	1.295 (0.899-1.867)	0.165	-	-
Neural Invasion (Yes vs No)	1.123 (0.784-1.608)	0.526	-	-
Chemotherapy (Yes vs No)	0.580 (0.403-0.853)	0.003	0.761 (0.524-1.105)	0.151
SIRT5 expression (High vs Low)	0.590 (0.411-0.847)	0.004	0.669 (0.462-0.970)	0.034

656 Univariate and multivariate Cox proportional hazards regression were used to calculate Hazard ratio
657 (HR), 95% confidence intervals (95% CI) and *p* values in SPSS 22.0.
658

659 **Table S3. Univariate and Multivariate Analysis for the Prognostic Factors**
 660 **of Disease-Free Survival in PDAC Patients from Figure 1.**
 661

Variables	Univariate		Multivariate	
	Analysis	<i>P</i> value	Analysis	<i>P</i> value
	HR (95% CI)		HR (95% CI)	
Gender (male versus female)	1.313 (0.920-1.875)	0.134		
Age (≥62 years vs <62 years)	1.190 (0.842-1.683)	0.324		
pT status (T3 or T4 vs T1 or T2)	0.932 (0.648-1.341)	0.706		
pN status (N1-2 vs N0)	1.580 (1.115-2.239)	0.010	1.398 (0.492-3.977)	0.529
pM status (M1 vs M0)	1.302 (0.531-3.195)	0.564		
AJCC stage (III or IV vs I or II)	1.593 (1.125-2.256)	0.009	1.605 (1.130-2.277)	0.008
Histological grade (G3 vs G1 or G2)	1.413 (0.990-2.017)	0.057	1.451 (1.014-2.076)	0.042
Tumor size (≤4 cm vs >4 cm)	0.858 (0.604-1.218)	0.392	-	-
Recurrence (Yes vs No)	2.790 (1.807-4.308)	<0.001	2.572 (1.651-4.008)	<0.001
CEA (≥5 ng/mL vs <5ng/mL)	0.985 (0.697-1.392)	0.931		
CA199 (≥37 U/mL vs <37U/mL)	1.139 (0.804-1.613)	0.464	-	-
Location (Head vs Body/Tail)	1.211 (0.852-1.721)	0.286	-	-
Neural Invasion (Yes vs No)	1.142 (0.807-1.618)	0.454	-	-
Chemotherapy (Yes vs No)	0.587 (0.413-0.836)	0.003	0.773 (0.540-1.108)	0.161
SIRT5 expression (High vs Low)	0.505 (0.355-0.719)	<0.001	0.605 (0.423-0.864)	0.006

662 Univariate and multivariate Cox proportional hazards regression were used to calculate Hazard ratio
 663 (HR), 95% confidence intervals (95% CI) and *p* values in SPSS 22.0.

664

665 **Table S4. Primers used in this study.**

Oligonucleotides		
Primers for qPCR		
hSIRT5-F	Eurofins MWG Operons	GCCATAGCCGAGTGTGAGAC
hSIRT5-R	Eurofins MWG Operons	CAACTCCACAAGAGGTACATCG
hGLS-F	Eurofins MWG Operons	AGGGTCTGTTACCTAGCTTGG
hGLS-R	Eurofins MWG Operons	ACGTTTCGCAATCCTGTAGATTT
hGLS2-F	Eurofins MWG Operons	GCCTGGGTGATTTGCTCTTTT
hGLS2-R	Eurofins MWG Operons	CCTTTAGTGCAGTGGTGAACCT
hGLUD1-F	Eurofins MWG Operons	GGGCTTTTGTATCCGTTACAGC
hGLUD1-R	Eurofins MWG Operons	GGTCAAACGGCCATAGCTGA
hGOT1-F	Eurofins MWG Operons	ATGGCACCTCCGTCAGTCT
hGOT1-R	Eurofins MWG Operons	AGTCATCCGTGCGATATGCTC
hGOT2-F	Eurofins MWG Operons	AGCCTTACGTTCTGCCTAGC
hGOT2-R	Eurofins MWG Operons	AAACCGGCCACTCTTCAAGAC
hME1-F	Eurofins MWG Operons	GAGTGCTGACATCTGACATTGA

hME1-R	Eurofins MWG Operons	TTGGCTTCCGAAACACCAAAC
hMDH1-F	Eurofins MWG Operons	GGTGCAGCCTTAGATAAATACGC
hMDH1-R	Eurofins MWG Operons	AGTCAAGCAACTGAAGTTCTCC
h18S rRNA-F	Sigma-Aldrich	CTACCACATCCAAGGAAGCA
h18S rRNA-R	Sigma-Aldrich	TTTTTCGTCACTACCTCCCCG
Primer for genotyping		
Mice Kras ^{G12D} -Y116	Sigma-Aldrich	TCCGAATTCAGTGACTACAGATG
Mice Kras ^{G12D} -Y117	Sigma-Aldrich	CTAGCCACCATGGCTTGAGT
Mice Kras ^{G12D} -Y118	Sigma-Aldrich	ATGTCTTTCCCCAGCACAGT
Mice p53 ^{R172H} -T35	Sigma-Aldrich	CTTGGAGACATAGCCCACTG
Mice p53 ^{R172H} -T36	Sigma-Aldrich	CTCTGGAATTCGCAAGCTA
Mice p53 ^{R172H} -T37	Sigma-Aldrich	TTACACATCCAGCCTCTGTGG
Mice Pdx1-Cre-F	Sigma-Aldrich	CTGGACTACATCTTGAGTTGC
Mice Pdx1-Cre-R	Sigma-Aldrich	GGTGTACGGTCAGTAAATTTG
Mice Sirt5 ^{lox/lox} -F	Sigma-Aldrich	TGTGCTTGTACGTGCTGTGC
Mice Sirt5 ^{lox/lox} -R	Sigma-Aldrich	CCCCTCACTCAGCTCACAAA
Primers for site mutagenesis		
GOT1-sequence-F	Sigma-Aldrich (HPLC purified)	TGCCTGGGCCATTTCGCTATTTTG
GOT1-sequence-R	Sigma-Aldrich (HPLC purified)	TCACTGGATTTTGGTGACTGC
GOT1-K276R-F	Sigma-Aldrich (HPLC purified)	CGA GAA CCT GAG AGC ATC CTG CAA G
GOT1-K276R-R	Sigma-Aldrich (HPLC purified)	TCCAACCACAGTCAGATTCCCGAC
GOT1-K290R-F	Sigma-Aldrich (HPLC purified)	CGG ATC GTG CGG ATT ACT TGG TC
GOT1-K290R-R	Sigma-Aldrich (HPLC purified)	CTC CAT CTG GGA AAG GAC TTG CAG
GOT1-K369R-F	Sigma-Aldrich (HPLC purified)	CGG CAG GTT GAG TAT CTG GTC AAT G
GOT1-K369R-R	Sigma-Aldrich (HPLC purified)	GGG GTT CAA CCC AGT GAA GCT GAA C
sgGOT1-resistant-F	Sigma-Aldrich (HPLC purified)	G AGA AAG GTC AAC CTG GGA GTG
sgGOT1-resistant-R	Sigma-Aldrich (HPLC purified)	GGGTCCGGATCCTCCCTGAAG
SIRT5-H158Y-F	Sigma-Aldrich (HPLC purified)	TAT GGTAGCT TATTTAAAAC TCG

SIRT5-H158Y-R	Sigma-Aldrich (HPLC purified)	GATCTCCAGAAGGTTCTTGGTG
H158Y-sequence-F	Sigma-Aldrich (HPLC purified)	A TGCGACCTCT CCAGATTGTC
H158Y-sequence-R	Sigma-Aldrich (HPLC purified)	GGAAGTTTCTCAACTGGGATGCT

666